Baek, S. H., Moon, H. K., A study on the rock fracture mechanism of cutter penetration and the assessment system of TBM tunnelling procedure.
International Symposium on the Fusion Technology of Geosystem Engineering, Rock Engineering and Geophysical Exploration
Seoul, Korea, Nov. 18-19, 2003

# A study on the rock fracture mechanism of cutter penetration and the assessment system of TBM tunnelling procedure

Seung Han Baek, Hyun Koo Moon
Hanyang University, Seoul, Korea

Abstract: Excavation by TBM can be characterized by a rock-machine interaction during the cutting process on a small scale, but on a large scale the interaction between the rock mass and TBM becomes very significant. For the planning and evaluation of TBM tunnelling it needs to understand rock fracture mechanism by a cutter or cutters on a small scale, and to estimate penetration rate, advance rate and utilization on a large scale. In this study rock chipping mechanism due to cutter-penetration is analysed by numerical simulation, showing that rock chipping is mainly occurred by tensile failure. Also, through the analysis of factors that affect on TBM procedures in various assessment systems, it is determined that the key elements that should be considered in the planning and evaluation of TBM tunnelling are classified into rock properties, the geological structures and properties of rock mass, and the structural and functional specifications of the machine. The user-friendly assessment tool is developed, so that penetration rate, advance rate and TBM utilization are evaluated from various input data. The tool developed in this study can be applied to a practical TBM tunnelling by understanding TBM tunnelling procedures.

## 1. Introduction

Rock excavation by using a cutter is the effective rock fragmentation technique, and is widely applied to not only mining but also mechanical tunnel excavation. On a small scale, excavation by TBM can be characterized by a rock-machine interaction during the cutting process, but the interaction between the rock mass and TBM becomes very important on a large scale as shown in Fig. 1 (Moon, 2001).

Locally concentrated high stresses in a rock are occurred by cutter penetration, and microcracks propagate, interact, coalesce and finally form rock chips. This is caused by the local concentration of tensile stress due to heterogeneity of rock. As the formation and growth of cracks are irreversible and cumulative, it is often observed that the secant elastic modulus of rock degrades gradually as the cracking events increase (Fang and Harrison, 2001; Liu et al., 2002).

The rock fracture mechanisms are influenced by many factors, among which confining pressure is one of the most important. As a result, when confining pressure varies, the strength and stiffness degradation of the rock significantly change by fracturing. With increasing confining pressure, the peak and ultimate strengths of the rock increase, whilst the strength loss after peak decreases. Thus chipping processes of rock must be analysed by considering rock heterogeneity and degradation of rock properties after failure.

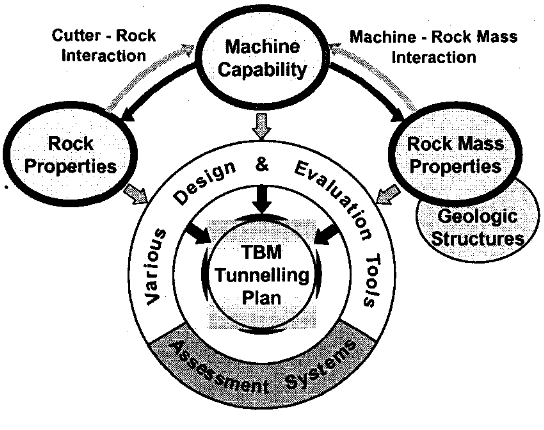

Fig. 1. TBM tunnelling plan.

Three key elements that should be considered in the planning and evaluation of TBM tunnelling are 1) the properties of rock as material, 2) the geological structures and properties of rock mass, and 3) the structural and functional specifications of the machine (Moon, 2001). Engineers for TBM tunnelling may have various amounts of information on rock properties, and also obtain different levels of information on rock mass properties and conditions. The planning and evaluation of TBM tunnelling are not a passing work but a continuing task until the completion of tunnelling. Therefore the engineers need various design and evaluation tools appropriate for the information in their hands. To apply the assessment systems proposed by some researchers, a number of equations, charts and graphs must be used, and this seems to be very inconvenient and complicated.

For the planning and evaluation of TBM tunnelling, it needs to understand chipping mechanism of rock induced by cutter-penetration and to estimate penetration rate, advance rate and utilization. In this study, the numerical analysis for chipping processes of rock due to cutter-penetration is performed by using FLAC (Itasca, 1995). Also four assessment systems are introduced and analysed, and the user-friendly program is developed for the TBM tunnelling procedure.

## 2. Numerical Modelling for Cutter Penetration

Generally rock is a heterogeneous material that contains many cracks, and hence a more complex material behaviour is taken into account because homogeneous continuous elastic medium cannot capture the features of the rock fragmentation process induced by cutter-penetration. In this study, Weibull distribution function is applied for the heterogeneity of rock properties as follows:

$$p(x) = \frac{m}{x_0}\left(\frac{x - x_L}{x_0}\right)^{m-1} \exp\left[-\left(\frac{x - x_L}{x_0}\right)^{m}\right], \tag{1}$$

where $m$ is the shape parameter describing the scatter of $x$, $x_0$ is a scale parameter, and $x_L$ is the lower bound value of $x$.

Fig. 2 shows the shape of the probability density function with typical shape parameters when $x_0$ is 1 and $x_L$ is 0. The curve at $m = 1$ is similar to negative exponential distribution, and the material becomes more homogeneous as $m$ increases.

As mentioned earlier, rock fracture mechanisms and degradation of rock properties are influenced by confining pressure. During cracking processes a rock shows non-linear behaviour and degradation of strength significantly changes. In particular, rock often displays a brittle behaviour and suffers the maximum degradation in uniaxial compression.

The elastic strain-softening behaviour can be considered as being a combination of both brittle and ductile components. By Fang and Harrison (2001, 2002), it is assumed that the brittle component is associated with microcracking processes, and it produces no plastic strain and results only in reduction in material stiffness and strength. On the other hand, the ductile component produces plastic strain but has no effect on either stiffness or strength. Through these assumptions and by using Fig. 3, the degradation index of rock can be defined as follows:

$$r_d = \frac{\sigma - \sigma_d}{\sigma - \sigma_{dh}} = \frac{\delta\sigma}{\delta\sigma_h}, \tag{2}$$

where $\sigma_c$ is uniaxial compressive strength, and the strength degradation $\sigma_c - \sigma_{du} = \delta\sigma_u$ represents the maximum degradation for the uniaxial case. For the general case, the degraded stress-strain curve would be as shown by the curve entitled 'hypothetical degradation', and degraded strength would be $\sigma_{dh}$. The degraded strength for the general case is $\sigma_d$, and hence the ratio between the general strength degradation, $\delta\sigma$, and hypothetical degradation, $\delta\sigma_h$, is the degradation index. The degradation index is influenced by confining pressure and ranges from 0 to 1, and can represent brittle, quasi-brittle and ductile behaviour. The degradation index is zero in no degradation and the degradation index is 1 in case of complete degradation.

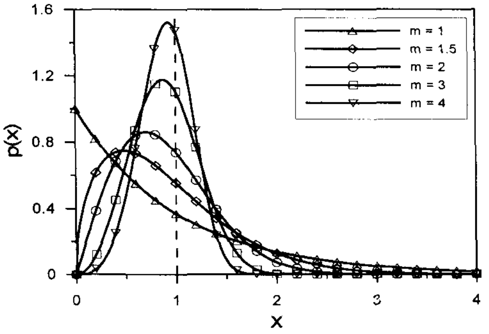

Fig. 2. The Weibull distribution function for various values of shape parameter.

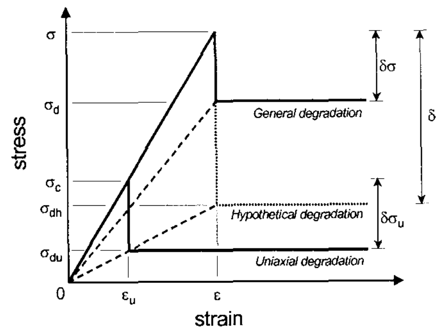

Fig. 3. Illustration of the definition of the degradation index (Fang and Harrison, 2001).

A simple equation may be proposed for the relationship between degradation index and confining pressure from laboratory test data as follows:

$$r_d = \exp(-n_d \sigma_3), \qquad (3)$$

where $\sigma_3$ is minor principal stress, and the parameter $n_d$ describes either the linearity or the curvature.

In order to analyse rock chipping processes due to cutter-penetration, the domain of single cutter-penetration model is (200×100) and that of double cutter-penetration model is (250×100) as shown in Fig. 4. Here, Young's modulus is 40 GPa, Poisson's ratio is 0.25, uniaxial compressive strength is 200 MPa, brittleness ratio is 20 and internal friction angle is 35 ° as summarized in Table 1.

In the current simulations, shape parameter $m$ = 2 is used on the basis of Weibull distribution and cut-off Mohr-Coulomb failure criterion is applied. Cutter penetration increment is 0.005 mm/step and a confining pressure is applied on both the lateral sides.

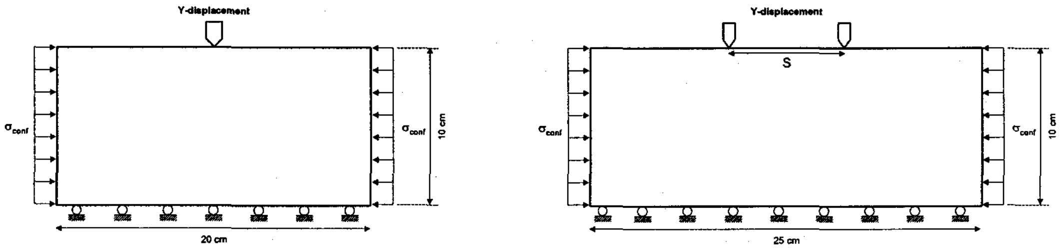

(a) Single cutter (b) Double cutter

Fig. 4. Numerical simulation model.

Table 1. Material properties used in numerical analysis.

| | |
|---|---|
| Young's modulus, E | 40 GPa |
| Poisson's ratio, ν | 0.25 |
| Uniaxial compressive strength, $\sigma_c$ | $x_0$ = 200 MPa<br>$x_L$ = 50 MPa<br>m = 2 |
| Reciprocal of brittleness ratio, $T_0/\sigma_c$ | $x_0$ = 0.05<br>$x_L$ = 0<br>m = 2 |
| Internal friction angle, ϕ | 35 ° |
| Uniaxial degradation in strength, $\delta\sigma_u$ | 90 % |
| Degradation parameter, $n_d$ | 0.05 |

## 3. Rock Failure due to Cutter-Penetration

### Effect of confining pressure in single cutter-penetration

Fig. 5 shows failure zones with respect to the confining pressure in single cutter penetration. Generally tensile failure occurred at the corners of cutter first, which seems to be because the tensile strength of brittle rock is much lower than the compressive strength, and then with loading step increasing, the rock immediately beneath the cutter fails. The failure zones of both sides have no symmetric shapes and propagate in a curvilinear path, which seems to be caused by the heterogeneity of rock. As the confining pressure increases, the chips formed by cutter penetration become larger. The side failure zone initiated from area around the cutter is driven by tensile stress to propagate in curvilinear paths and finally intersect with the free surface of the rock to form chips. Therefore the mechanism causing chipping process is mainly tensile failure.

The horizontal failure zone and vertical failure zone induced by cutter penetration is shown in Fig. 6. The horizontal failure zone represents the maximum size of chips to be formed. As the confining pressures increase from 10 MPa to 50

MPa in steps of 20 MPa, the horizontal maximum failure zone is 3.8 cm, 4.9 cm, 5.8 cm at 1 mm penetration, 5.5 cm, 6.0 cm, 9.1 cm at 2 mm penetration and 6.8 cm, 7.7 cm, 13.8 cm. The vertical failure zone decreases as confining pressure increases, showing vertical maximum failure zone is 1.9 cm, 1.4 cm and 1.1 cm when the confining pressure is 10 MPa, 30 MPa and 50 MPa at 3 mm penetration.

(a) $\sigma_{conf}$ = 10 MPa (b) $\sigma_{conf}$ = 30 MPa (c) $\sigma_{conf}$ = 50 MPa

Fig. 5. Failure zone with respect to confining pressure.

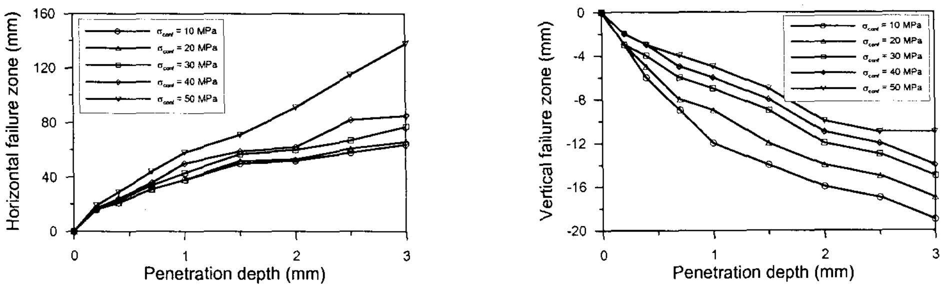

(a) Horizontal failure zone (b) Vertical failure zone

Fig. 6. The maximum failure zone with penetration depth.

## Effect of cutter spacing in double cutter-penetration

At confining pressure of 50 MPa, the aspects of failure zones when cutter spacing S is 40 mm, 70 mm and 100 mm is shown in Fig. 7. In case of S = 40 mm, the failure zone coalesces immediately between cutters but does not fully propagate up to the rock surface. At S = 70 mm, the tensile failure around the two corners of both cutters and shear failure beneath both cutters occurred, and the failure zones between cutters connect each other. Also, the rock chips including the elastic parts between both cutters are formed as loading step continues. When S is 100 mm, the failure zones around both cutters do not intersect each other and the rock between cutters remains elastic because cutter spacing is relatively wide. This is unfavorable because high cutter thrust must be applied continuously to connect failure zones of both sides.

The failure area is larger at S = 70 mm than S = 40 mm and 100 mm, implying coalescing processes of failure zones on cutter spacing have an important influence on rock fragmentation. On the other hand, cutter spacing has no influence on vertical failure zone. When cutter penetration is 1 mm, 2 mm and 3 mm, horizontal failure zone is 9.3 mm, 10.5 mm and 11.5 mm at S = 40 mm, and 14 mm, 14.3 mm and 14.8 mm at S = 70 mm. In case of S = 100 mm, the failure zones of both sides do not intersect each other.

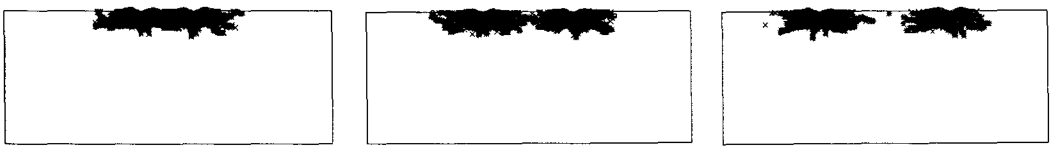

(a) S = 40 mm (b) S = 70 mm (c) S = 100 mm

Fig. 7. Failure zone with respect to cutter spacing.

## 4. Development of TBM Tunnelling Assessment System

TBMs are normally manufactured on the basis of a specified range of rock and rock mass conditions of given tunnel projects. This may be called "forward path", since the size and capacity of the machine is designed for the project's requirements. The other is "reverse path" which is to apply used TBMs to new tunnel projects. Recently the demand for reutilization of used TBMs increases as the number of new tunnel projects increases.

In this study, four assessment systems proposed by Persson et al. (1993), NUST (NTH, 1994; Bruland, 1998), Jodl and Stempkowski (1996), and Barton (1999, 2000) are analysed and compared for the TBM tunnelling procedures. These systems are inconvenient to apply because a number of equations, charts and graphs are used. Therefore the program based on Windows system that may be applied easily by engineers, is developed as shown in Fig. 8. The developed program is convenient to apply to each system consistent with input data. In spite of the lack of some pre-requisite data, the prediction and evaluation is possible if there are the minimum data for calculation. For detailed calculation steps for these systems, see the references.

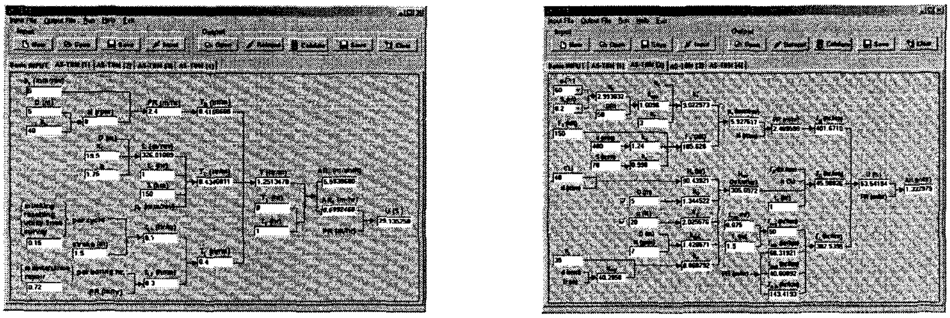

(a) assessment system [1]

(b) assessment system [2]

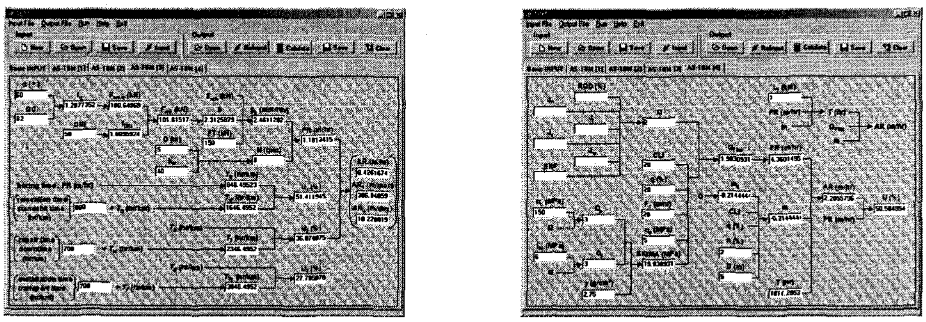

(c) assessment system [3]

(d) assessment system [4]

Fig. 8. Assessment systems for TBM tunnelling procedure.

### Assessment system [1]

This assessment system is reconstructed and modified from one by Persson et al. (1993). Penetration rate PR is calculated form cutterhead diameter D, penetration depth $p_e$ and cutterhead rotation rate factor $k_N$ among twelve input data, and then the time required to bore a tunnel meter is determined. The time to change disc cutters is predicted from cutterhead diameter, coefficients to calculate total path length $k_C$ and a, average time required to change a single cutter $t_C$ and cutter lifetime $\lambda$, and total loss time $T_L$ is calculated from data such as loss time per cycle, stroke $l_s$, loss time per boring time and penetration rate. From these times, advance rate AR and utilization U is determined finally.

### Assessment system [2]

This section describes the prognosis model for TBM tunnelling developed by the Norwegian University of Science and Technology (NTH, 1994; Bruland, 1998). The model is based on two groups of parameters; one is for the rock mass to be excavated and the other is for the TBM. The basic input data of this system are drilling rate index DRI, cutter life index CLI, quartz content q, angle between the tunnel axis and weakness planes $\alpha$, fracture class FC, total number of joint sets $n_f$, cutter thrust $F_T$, cutter diameter d, cutter spacing S, the number of cutters $n_C$, cutterhead diameter D, cutterhead rotation rate N, stroke length $l_s$ and the time for regripping $t_{reg}$. Among these data, the most important factors defining the rock mass conditions for TBM tunnelling include 1) equivalent fracturing factor $k_f^*$, 2) drilling rate index, and 3) cutter life index. After penetration depth is calculated from equivalent fracturing factor and equivalent cutter thrust $F_T^*$, penetration rate can be predicted. TBM Utilization is evaluated from boring time $T_B$, cutter change time $T_C$ and total loss time $T_L$, and advance rate is predicted from the relation between penetration rate and utilization.

### Assessment system [3]

This section describes the assessment system proposed by Jodl and Stempkowski (1996). The basic input data of this model are drilling rate index DRI, angle between the tunnel axis and weakness planes $\alpha$, ground condition GC, cutter thrust $F_T$, cutterhead diameter D, cutterhead rotation rate factor $k_N$, relocation time, standstill time, repair time, downtime, installation time and transport time. Penetration depth is predicted from maximum cutter thrust, ground condition and drilling rate index, and then penetration rate is determined from Penetration depth, cutterhead rotation rate factor and cutterhead diameter. On the basis of the boring time $T_B$, total working time which include the time for boring, relocation, and standstill except for the repair time and downtime $T_W$, total tunnelling time except for the installation time and transport time $T_T$, total commission time including the time for installation and transport $T_{T+}$, and penetration rate, utilization is calculated. Advance rate can be then estimated on the penetration rate and utilization $U_2$.

### Assessment system [4]

In this assessment system proposed by Barton (1999, 2000), a new index $Q_{TBM}$ for TBM tunnelling is used by modifying the conventional rock mass quality index Q. The basic input data consist of rock quality index Q, uniaxial compressive strength of rock $\sigma_c$, point load strength of rock $I_{50}$, rock density $\chi$, quartz content q, cutter life index CLI, average cutter thrust force $F_T$, induced biaxial stress on tunnel face $\sigma_\theta$, cutterhead diameter D, and tunnel length $L_t$. Penetration rate is predicted from the properties of rock, the conditions of rock mass and cutter thrust, and then advance rate and utilization are evaluated from the rock quality index, penetration rate, and so on.

## 5. Analyses and Application of Assessment System

The parametric analyses are performed with changing the input parameters within the ranges as summarized Table 2. If one of the parameters is changed, then others are fixed at reference values.

In case of system [1], the effect of $p_e$ and D among various input parameters is large, and PR and AR increase but U decreases as $p_e$ increases. PR and AR decrease as D increases. On the other hand, U increases with increasing D, and reaches the maximum value at D = 6 m, and then decreases.

As the results of the analysis on system [2], the important parameters are $\alpha$, $S_f$, $F_T$ and D. At every fracture classes PR and AR is maximum and U is minimum in case of that $\alpha$ is $60^\circ$. When $S_f$ is 50 cm, 80 cm and 160 cm, PR is 2.52 m/hr, 1.28 m/hr and 0.39 m/hr, and AR decreases from 1.35 m/hr, 0.82 m/hr to 0.31 m/hr but U increases from 53.4 %, 63.8 % to 78.9 % as shown in Fig. 9. $F_T$ has a contrary influence on PR, AR and U in contrast to $S_f$.

Through the parametric analysis of system [3], the input variables that have a great influence on PR, AR and U are $F_T$, D, GC and $\alpha$. PR and AR increase as $F_T$ increases and D decreases, whereas U decreases as $F_T$ decreases and D increases

PR, AR and U is largely influenced by $F_T$, Q and q in the system [4]. PR decreases as Q increases, and AR is the maximum at Q of 1, and U is the maximum when Q is 10 as shown in Fig. 10. As $F_T$ increases, PR and AR increases but U is constant.

In this study the data of Youngchun water tunnel project in Korea are analysed, and the purpose of this project can be summarized into two aspects: one is to expand water-supply capacity of Youngchun dam to meet the increasing demand in the south-east area of Kyungbuk Province. The other is to improve the water quality of the today very contaminated Kumho river. The TBM (ATB 35) for this project was manufactured by VOEST-ALPINE BERGTECHNIK and has 24 cutters, the diameter of which is 3.5 m.

As shown in Fig. 11, the average penetration rate PR is 1.93 m/hr, the advance rate AR is 0.41 m/hr and the average utilization U is about 21 %. These values are very low, and this is caused by the rest times excluding the times such as downtime, transport time and time for meals. Therefore it is desirable to analyse penetration rate PR than advance rate AR or utilization U in the case of mentioned above.

Table 2. Input data for parametric study.

| System [1] | | System [2] | | System [3] | | System [4] | |
|---|---|---|---|---|---|---|---|
| parameter | range | parameter | range | parameter | range | parameter | range |
| $p_e$ (mm/rev) | 2~10 | α (°) | 0~90 | α (°) | 0~90 | Q | 0.001~1000 |
| D (m) | 3~15 | $S_f$ (m) | 0.05~1.6 | GC | B1~C2 | $\sigma_c$ (MPa) | 20~300 |
| λ (km) | 100~500 | DRI | 10~90 | DRI | 10~90 | $I_{50}$ (MPa) | 0.2~50 |
| $k_N$ | 30~50 | CLI | 10~130 | $F_T$ (kN) | 100~250 | χ (g/cm$^3$) | 2~3 |
| | | $F_T$ (kN) | 100~250 | D (m) | 2~13 | CLI | 10~130 |
| | | D (m) | 2~13 | $k_N$ | 30~50 | q (%) | 5~100 |
| | | | | | | $F_T$ (tonf) | 10~35 |
| | | | | | | $\sigma_\theta$ (MPa) | 2~20 |
| | | | | | | n (%) | 0.5~5 |
| | | | | | | D(m) | 3~13 |

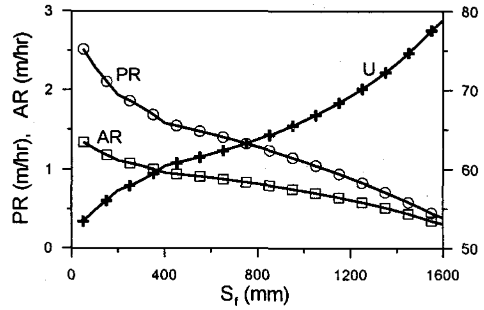

Fig. 9. PR, AR and U with $S_f$ in system [2].

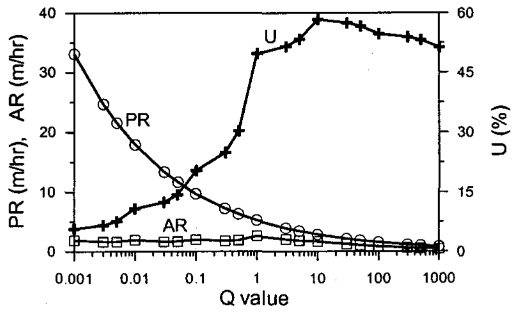

Fig. 10. PR, AR and U with Q value in system [4].

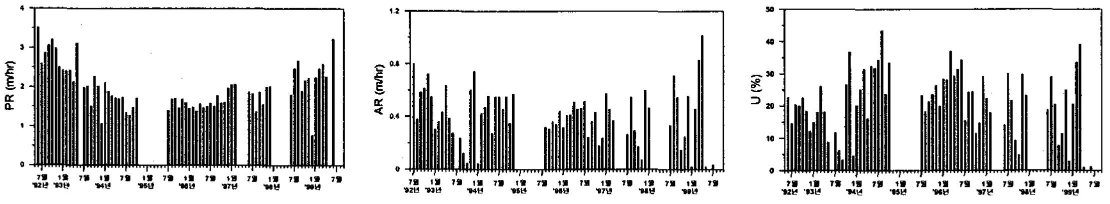

(a) Penetration rate

(b) Advance rate

(c) Utilization

Fig. 11. The results of Youngchun water tunnel project.

## 6. Conclusions

In this study, rock chipping processes due to cutter-penetration are analysed by using Weibull distribution function and degradation index to consider the heterogeneity and strength degradation of rock after peak. Assessment systems for TBM tunnelling procedure are compared and a user-friendly program is developed in order to estimate TBM tunnelling performance. The tool can be applied to a practical TBM tunnelling through understanding of TBM tunnelling procedures.

In single cutter-penetration, shear failure occurs beneath the cutter as the confining pressure becomes lower, but the larger chips is formed at the both side by tensile stresses as confining pressure increases. It is analysed that cutter spacing is one of the most important factors on chipping process as the results of double cutter-penetration simulations.

Also four assessment systems are introduced and discussed with detailed input parameters. The factors that have an influence on TBM tunnelling performance are penetration depth $p_e$ and TBM diameter D in system [1], fracture spacing $S_f$, cutter thrust $F_T$, angle between the tunnel axis and weakness planes $\alpha$ and TBM diameter D in system [2], cutter thrust $F_T$, TBM diameter D, quartz content q and angle between the tunnel axis and weakness planes $\alpha$ in system [3], and cutter thrust $F_T$, rock quality index D, quartz content q and cutter life index CLI in system [4].

Suitable for the design and planning of TBM tunnelling before field operation are the system [2] and [4], where PR, AR, U and T are estimated directly from known rock properties, rock mass conditions and disc cutter data. On the other hand, The system [1] and [3] are suitable for post-evaluation of TBM performance because the data on various loss time should be obtained from TBM operation in the field.

This study will help to plan and evaluate the TBM tunnelling by understanding the chipping processes of rock induced by cutter-penetration and by using the user-friendly program tool developed on the basis of four assessment systems.

## References

Barton, N, 1999, TBM Performance Estimation in Rock Using $Q_{TBM}$, Tunnels & Tunnelling International, Vol. 31, No. 9, pp 30-34.

Barton, N., 2000, TBM Tunnelling in Jointed and Faulted Rock, Balkema, p. 172.

Bruland, A., 1998, Prediction Model for Performance and Costs, Norwegian TBM Tunnelling, Norwegian Soil and Rock Engineering Association, Publication No. 11, pp. 29-34.

Fang, Z. and Harrison, J.P., 2001, A mechanical degradation index for rock, International Journal of Rock Mechanics & Mining Sciences, Vol. 38, pp. 1193-1199.

Fang, Z. and Harrison, J.P., 2002, Development of a local degradation approach to the modelling of brittle fracture in homogeneous rocks, International Journal of Rock Mechanics & Mining Sciences, Vol. 39, pp. 443-457.

Itasca, 1995, Fast Lagrangian Analysis of Continua, Version 3.3, Minnesota.

Jodl, H.G. and Stempkowski, R., 1996, Operations Research Aspects of TBM Drives-Case Study of the Wienerwald tunnel, Proc. Int. Lecture Series TBM Tunnelling Trends, Austria, pp. 69-79.

Liu, H.Y., Kou, S.Q., Lindqvist, P.A. and Tang, C.A., 2002, Numerical simulation of the rock fragmentation process induced by indenters, International Journal of Rock Mechanics & Mining Sciences, Vol. 39, pp. 491-505.

Moon, H.K., 2001, A Comparative Study on Five Assessment Systems of TBM Tunnelling, Geosystem Engineering, 4(2), pp. 61-69.

Moon, H.K., 2001, A Study on the Assessment System of TBM Tunneling Procedure, The International Symposium on Application of Geosystem Engineering, p. 93-104.

NTH, 1994, Hard Rock Tunnel Boring, Project Report 1-94, p. 164.

Persson, P., Holmberg, R. and Lee, J., 1993, Rock Blasting and Explosives Engineering, CRC Press, pp. 43-53.